The hadronic models for cosmic ray physics: the FLUKA code solutions

G. Battistoni[a], M.V. Garzelli[a*], E. Gadioli[a], S. Muraro[a], P.R. Sala[a], A. Fassò[b], A. Ferrari[c], S. Roesler[c], F. Cerutti[c], J. Ranft[d], L.S. Pinsky[e], A. Empl[e], M. Pelliccioni[f] and R. Villari[g]

[a]INFN, Sezione di Milano and Università di Milano, Dip. di Fisica, via Celoria 16, I-20133 Milano, Italy

[b]SLAC, Stanford, CA 94025, US

[c]CERN, CH-1211 Geneva 23, Switzerland

[d]Siegen University, Fachbereich 7 - Physik, D-57068 Siegen, Germany

[e]University of Houston, Department of Physics, TX 77204-5005 Houston, US

[f]INFN, via Fermi 40, I-00044 Frascati (Rome), Italy

[g]ENEA, via Fermi 45, I-00044 Frascati (Rome), Italy

FLUKA is a general purpose Monte Carlo transport and interaction code used for fundamental physics and for a wide range of applications. These include Cosmic Ray Physics (muons, neutrinos, EAS, underground physics), both for basic research and applied studies in space and atmospheric flight dosimetry and radiation damage. A review of the hadronic models available in FLUKA and relevant for the description of cosmic ray air showers is presented in this paper. Recent updates concerning these models are discussed. The FLUKA capabilities in the simulation of the formation and propagation of EM and hadronic showers in the Earth's atmosphere are shown.

1. Introduction

Extended Air Showers (EAS) are originated by highly energetic cosmic rays, which interact with air atoms in the Earth's atmosphere, producing elementary hadrons and nuclear fragments. Neutral pions immediately decay in two photons, which in turn interact with other particles, generating electromagnetic cascades, while charged pions and kaons, as well as other hadrons, interact and/or decay, depending on their energy and air density, leading to the hadronic component of the shower. Thus, to understand a process as complex as an air shower, models and codes capable of describing the evolution of both the electromagnetic and the hadronic component are needed. Monte Carlo codes have been developed in the last few years for this purpose, such as

the CORSIKA simulation package [1], allowing to choose among different models and model combinations for the description of EAS formation and propagation.

In this paper, the FLUKA Monte Carlo code [2, 3] is applied to the study of EAS induced by cosmic rays with primary energies up to 1000 TeV. These results rely entirely on the use of the FLUKA code for transport, interactions and decays of leptons and γs at all energies and for hadron-nucleus interactions at energies below 20 TeV, while the DPMJET code [4,5] is used for all nucleus-nucleus interactions and for hadron-nucleus interactions at the highest energies. Our simulations are completely independent with respect to CORSIKA, which contains only a partial version of FLUKA, for use at low energies only (E $\lesssim$ 100–200 GeV). The energy range spanned in this work is of interest for cosmic ray experiments aiming at the determination of the primary spectra and composition for energies up to the knee

---

*Correspon. author, *e-mail*: `Maria.Garzelli@mi.infn.it`
Invited talk presented at ISVHECRI 2006, International Symposium on Very High Energy Cosmic Rays, Weihai, China, August 15 - 22, 2006

arXiv:hep-ph/0612075 v1   7 Dec 2006

region, such as the ATIC, the RUNJOB and the KASCADE experiments.

It is worth mentioning that FLUKA has not been specifically designed for the study of Cosmic Ray Physics, but can be applied also in this field. At energies < 30 TeV, interesting results concerning the prediction of inclusive lepton fluxes have already been obtained. In particular, the first 3-dimensional calculation of the atmospheric neutrino flux due to Cosmic Rays [6] was made with FLUKA, and, more recently, data concerning muons detected by the balloon-borne BESS spectrometer at various depths and by the L3+C spectrometer located at CERN have been quite succesfully reproduced [7].

2. Validation of the FLUKA models

In this section some aspects of the FLUKA models relevant for Cosmic Ray description are briefly discussed, together with the validation of the models by means of data collected at accelerators. Actually, even the most recent accelerator data allow to test theoretical Monte Carlo models only for some specific projectile beam - target combinations at energies well below the maximum primary energies, while, for the simulation of EAS processes, one has to extrapolate the models to many more combinations and to the highest energies, on the basis of theoretical considerations.

2.1. FLUKA: a brief introduction

The modern FLUKA [2,3] is a general purpose Monte Carlo transport and interaction code developed since 1988 mostly by INFN and CERN researchers, and used in many fields of physics, both for fundamental research and for applications. The history of the code dates back to the sixties when J. Ranft developed and applied the very first version to accelerator shielding. The most common FLUKA applications are accelerator physics, calorimetry, shielding design, radioprotection and dosimetry, while new ones, such as hadrontherapy, are promisingly growing. Since a few years, FLUKA is also applied to Cosmic Ray Physics, mainly with focus on low energy cosmic rays, as already mentioned in the Introduction,
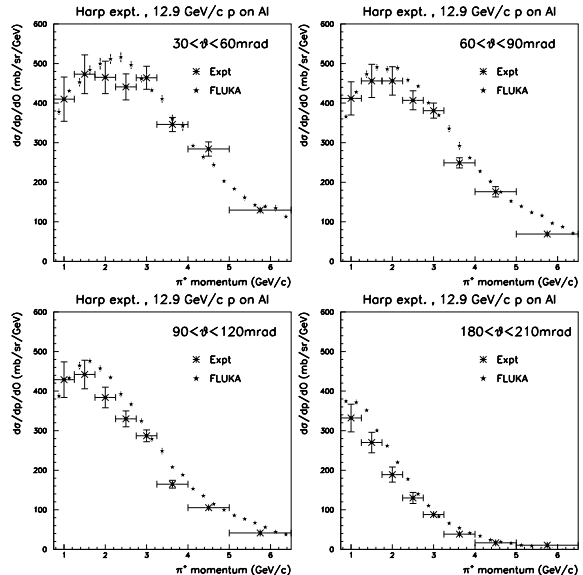

Figure 1. Computed π^+ double differential production cross section for 12.9 GeV/c protons on Aluminum for different angular ranges, compared with HARP experimental data [19].

and on their effects for dosimetry [8,9] and space physics [10]. All these applications require both precise physics models, and packages to build geometries, to simulate targets and experimental setups. Both topics are the subject of constant development and improvement in FLUKA.

As far as the geometry is concerned, a combinatorial geometry package is included into the code, allowing to create complex geometries, which can be visualized by means of apposite graphical tools. This allows to simulate 3-D particle propagation, and, as far as Cosmic Rays are concerned, to study showers characterized by whichever inclination angle and direction with respect to the Earth, and to take into account in a precise way the effect of different atmospheric compositions and magnetic field configurations. The same code can be used for the simulation of cosmic ray detectors, including surrounding materials.
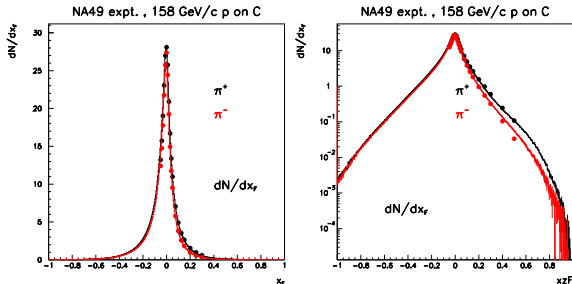
The FLUKA physical models are based as far

Figure 2. Feynman X distributions for π^+ and π^- production for proton interactions on Carbon at 158 GeV/c , as measured by NA49 [20] (symbols) and predicted by FLUKA (histograms). Linear scale on the left, logarithmic scale on the right.

as possible on theoretical microscopic models, with the advantage, with respect to parameterized inclusive models, of preserving correlations, and of being predictive in the regions where experimental data are not available. The model parameters are fixed once, internally to the code, for all projectile-target combinations and energies, and cannot be modified by the user. The theoretical models are continuously benchmarked against newly available experimental data. The code is under continuous development and made available on the website *http://www.fluka.org*. The development and maintenance are performed under a INFN–CERN agreement.

2.2. E.M. and muon transport in FLUKA

For historical reasons, FLUKA is best known for its hadron event generators, but since more than 17 years FLUKA can handle with similar or better accuracy electromagnetic effects [11]. Briefly, the energy range covered by this sector of FLUKA is very wide: the program can transport photons and electrons over about 12 energy decades, from 1 PeV down to 1 keV. The e.m. part is fully coupled with the hadron sector, including the low energy (i.e. < 20 MeV) neutrons. The simulation of the electromagnetic cascade in FLUKA is very accurate, including the Landau-Pomeranchuk-Migdal effect and a spe-

cial treatment of the tip of the bremsstrahlung spectrum. Electron pairs and bremsstrahlung are sampled from the proper double differential energy-angular distributions improving the common practice of using average angles. In a similar way, the three-dimensional shape of the hadronic cascades is reproduced in detail by a rigorous sampling of correlated energy and angles in decay, scattering, and multiple Coulomb scattering.

Bremsstrahlung and direct pair production by muons are modelled according to state-of-the-art theoretical description and have been checked against experimental data [12,13]. Muon photonuclear interactions are also modelled.
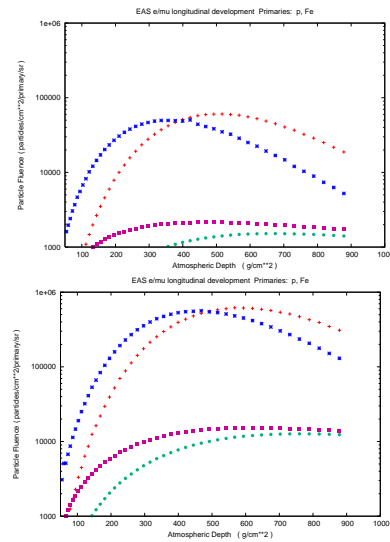
2.3. The FLUKA hadronic models

Figure 3. Average e/μ fluence as a function of the atmospheric depth for vertical showers induced by p, Fe primaries with 10^{14} eV (upper panel) and 10^{15} eV (lower panel) energies. In each figure e from Fe (asterisks), e from p (+ symbols), μ from Fe (filled squares) and μ from p (filled circles) are shown. The plots refer to e in the energy range 1 MeV - 1 TeV and to μ in the energy range 1 GeV - 1 TeV.

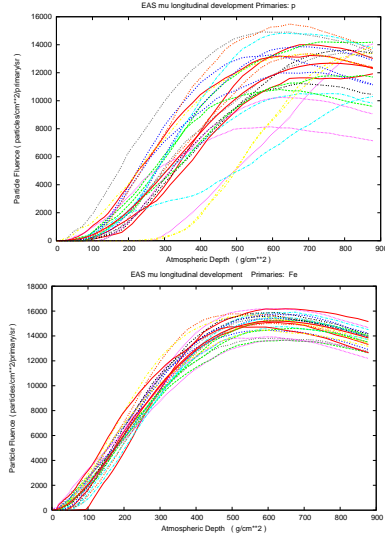Figure 4. μ fluence as a function of the atmospheric depth for vertical showers induced by p (upper panel) and Fe (lower panel) primaries with 10^{15} eV energy. Each line in each figure is the result for a different shower. In case of p showers, the development of the hadronic component shows larger fluctuations, also related to the depth of the first interaction. See also Fig. 3.

Figure 5. Spatial distribution of e fluence (particles/cm^2/primary) for vertical showers induced by Fe primaries with 10^{13} eV (upper panel) and 10^{15} eV (lower panel) energies. The results are obtained as an average on ~ 100 events for each energy. The primaries come from the top of the atmosphere (top of each figure) and propagate towards the Earth's surface located at ~ 6378 km with respect to the Earth's center.

A basic description of hadronic interactions in FLUKA can be found in [14]. Hadron-nucleon interactions at energies below a few GeV are simulated in FLUKA by the isobar model, through resonance production and decay, and by taking into account elastic, charge and strangeness exchange. Elementary hadron-hadron collisions at energies above a few GeV are described thanks to an implementation of the Dual Parton Model (DPM) [15], coupled to a hadronization scheme. The Dual Parton Model allows for the description of soft collision processes (i.e. processes characterized by low p_T, $p_T << Q_0$, where Q_0 is a momentum scale of the order of a few GeV), that cannot be described by means of pQCD, due to fast rise of α_S with decreasing momentum. DPM incorporates analiticity, duality and unitarity. Incoming hadrons are described by strings, whic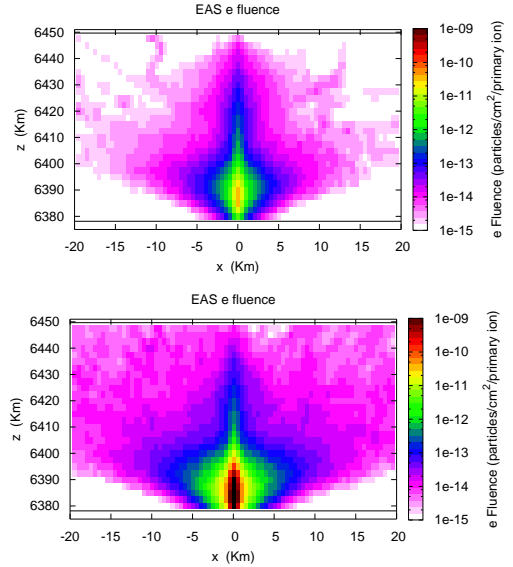h interact by exchanging closed loop excitations, called pomerons. At low energies, the single-pomeron exchange is the dominant contribution, while at laboratory energies $>> 1$ TeV higher-order contributions, corresponding to multi-pomeron exchange, become increasingly important. Corresponding to each pomeron cut, built according to the recipes provided by the Abramoviskii-Gribov-Kancheli cutting rules, colorless chains are built, extending from the projectile valence and sea quarks and antiquarks to the target ones. In particular, the valence quarks in each baryon are treated as a quark-diquark pair, so that, in the simplest case of the single-pomeron exchange amplitude for a baryon-baryon interaction, two chains are built, each extending from a valence quark to a valence diquark. Sea quarks (and the corresponding antiquarks) are additio-
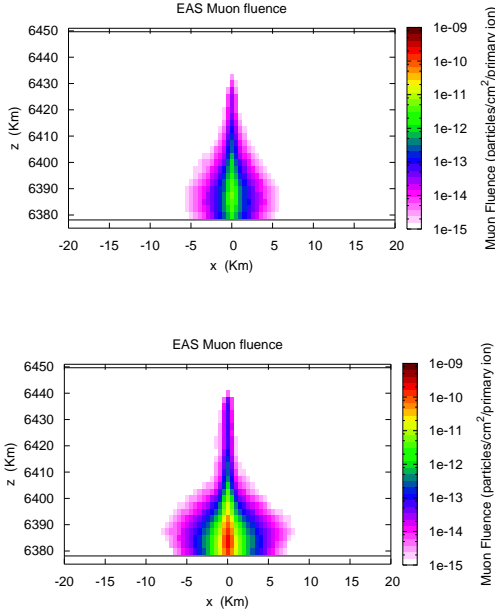
Figure 6. Same as Fig. 5 for μ fluence (particles/cm^2/primary) in vertical showers induced by Fe primaries with 10^{13} eV (upper panel) and 10^{15} eV (lower panel) energies.

Figure 7. Spatial distribution of EM energy deposition (GeV/cm^3/primary) for vertical showers induced by Fe ion primaries with 10^{13} eV (upper panel) and 10^{15} eV (lower panel) incoming energies. See also Fig. 5.

nally involved as end-points of chains in multi-pomeron exchange amplitudes. Besides determining the number of pomeron cuts and forming the chains, the DPM allows to assign an energy and momentum to each chain, according to the momentum distribution functions of the partons in the hadrons. In the asymptotic regime parton masses are neglected, however, at lower energies, finite mass effects have to be included both in the chain building process, by suppressing the chains with invariant masses below the observed baryon and meson mass values and reassigning energy and momentum to other chains to ensure energy/momentum conservation, and in the hadronization procedure. Hadronization is not included in DPM, but is performed by different models properly coupled to DPM. At present, the hadronization scheme implemented in FLUKA is based on an advanced version [16] of the model
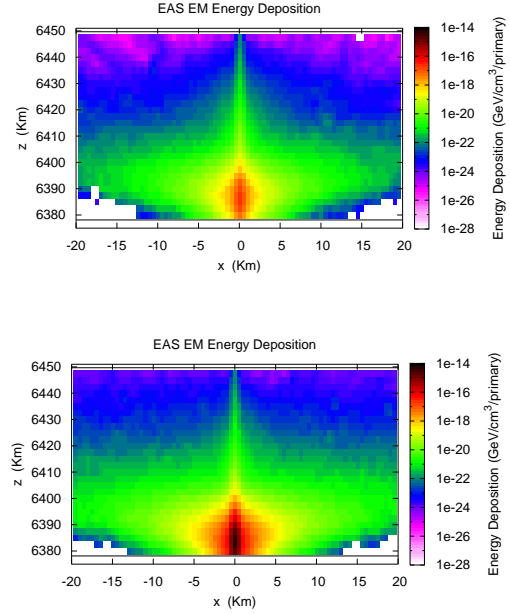
by [17], with special emphasis to provide accuracy in the low-energy description of hadron formation (down to a few GeV in the lab).

Hadron-hadron collisions are the main building blocks of hadron-nucleus collisions. Multiple collisions of each hadron with the nuclear constituents are taken into account by means of the Glauber-Gribov mechanism. Particular efforts are devoted to the study of nuclear effects on hadron propagation. In the last FLUKA version the propagation in the nucleus of the hadrons resulting from elementary multiple collisions can be simulated with improved accuracy with respect to the past, by means of an improved Generalized IntraNuclear Cascade (GINC) model, followed by pre-equilibrium and coalescence and by de-excitation of the remaining nuclear fragments. All these models are included in the FLUKA sub-

module PEANUT, which has been refined for several years to describe with increasing accuracy many low-energy processes involving nucleons, and has been further extended in the last few months to higher energy events (E > a few GeV). More detail about PEANUT and the issues concerning its extension can be found in [14,18]. PEANUT is used also to simulate γ, ν and stopping μ interactions, and nucleon decay. Photon interactions with hadrons and muon virtual photon nuclear interactions are simulated by means of the Vector Dominance Model.

Hadron free paths inside a nucleus can be different from those computed on the basis of free hadron-nucleon scattering, due to Pauli blocking, coherence length, formation and multibody processes, all implemented in FLUKA [14,18]. In particular, coherence length affects final states from elastic and charge-exchange scatterings: interaction products can not be localized better than the position uncertainty related to the 4-momentum transferred in the collision, according to the $\Delta x \Delta p \gtrsim \hbar$ relationship. Thus, reinteractions occurring at distances shorter than the coherence length undergo interference and can not be treated as independent. On the other hand, formation zone affects the reinteraction probability of secondaries emerging from high energy interactions. It is supported by experimental results, which indicate that high-energy secondary particle reinteractions inside nuclei are strongly suppressed. Taking into account that a typical time for strong interactions is ~ 1 fm/c, a particle emerging from an interaction requires some time to materialize, according to the uncertainty principle.

Examples of performance of the FLUKA hadronic model, in reproducing experimental data recently obtained by the HARP and NA49 Collaborations are shown in Fig. 1 and Fig. 2.

2.4. The FLUKA-DPMJET interface

Both hadronic physics at energies above 20 TeV and heavy-ion collisions above 5 GeV have been simulated in this work thanks to the interface of FLUKA with the DPMJET code. DPMJET-II.53 and DPMJET-III libraries can be both used within FLUKA. DPMJET is also available in
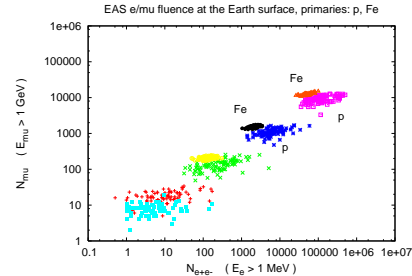

Figure 8. (N_e, N_μ) correlation at the Earth sea level: dependence on the primary mass and energy. Each symbol corresponds to a different shower event. Blobs from the lower left corner to the upper right corner refer to events originated from vertical p and Fe ions with initial energies 10^{12}, 10^{13}, 10^{14} and 10^{15} eV, respectively.
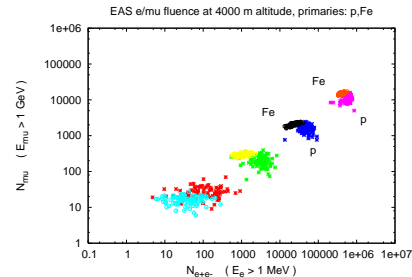

Figure 9. Same as Fig. 8 at a 4000 m a.s.l. altitude level. Calculations at such high altitudes are of interest for EAS experiments located at mountain sites.

CORSIKA as a possible choice among multiple high-energy event generators, and is widely used in the Cosmic Ray Physics community. DPMJET has been extensively tested against data from the SPS collider, the Tevatron and RHIC.

Soft physics is described in DPMJET [4,5] thanks to the DPM, already introduced in the previous section. Furthermore, hard physics processes are implemented, based on leading order pQCD. Soft and hard processes contribute together to the inelastic cross-section according to the eikonal approximation, which provides a uni-

tarization scheme. The eikonal function is given by the sum of the soft and hard components, also including terms from multi-pomeron exchange.

One of the main differences between the FLUKA hadronic physics models and DPMJET is related to the hadronization process. In DPM-JET this process is performed by means of the JETSET chain fragmentation code included in PYTHIA [21], with some modifications. In particular, while the PYTHIA code was extensively tested for processes involving a significant hard component, the transverse momentum distribution in soft chain decay has been modified in the JETSET version included in DPMJET to better describe soft chain hadronization. This way, the transverse momentum distributions of K and p predicted by DPMJET-III show an improved agreement with experimental data.

There are other differences in the description of final state interactions: DPMJET has its own GINC code, simplified with respect to the FLUKA one, and does not take into account coalescence and pre-equilibrium emission. Nuclear de-excitation is performed here by means of the same de-excitation models [14,22,23] used in FLUKA.

Further refinements of DPMJET and of its interface to FLUKA are under way. As an example, diquark breaking mechanisms, absent in the original DPM, have recently been proposed, in the attempt of providing a contribution to the enhanced stopping experimentally observed for nuclear collisions in fixed target experiments. The effects on the prediction of particle/antiparticle asymmetries, which can be compared with measured ones, are under investigation.

3. Theoretical EAS predictions

To test the capabilities of our model, we have simulated hundreds of vertical air shower events, for primary protons and iron nuclei, with energies in the $10^{12} - 10^{15}$ eV range. The average longitudinal EAS e/μ profiles are shown in the upper and lower panels of Fig. 3 for 10^{14} and 10^{15} eV primary energies, respectively. Electrons and positrons of energies ≥ 1 MeV have been considered, together with muons of energies ≥ 1 GeV,

up to 1 TeV. As can be seen from each figure, at a fixed energy, the X_{max}^e depth decreases with increasing primary mass, due to the behaviour of the p-air inelastic scattering cross-section, which indeed increases with mass number. The same is true also for $\mu^{\pm}$, whose longitudinal profile is however softer, i.e. has a maximum less peaked than the $e^{\pm}$ one. More detail about the $\mu^{\pm}$ longitudinal development can be inferred from Fig. 4, where profiles relative to individual showers induced by p (upper panel) and Fe (lower panel) primaries at 10^{15} eV are shown. Profile fluctuations are more evident for lower mass primaries, also related to the location of the first primary interaction with air, which can even vary within a range of a few km for low mass primaries and low density atmosphere. The muon number reflects the development of the hadronic component of the shower, and is thus a basic test of the hadronic models, since muons come from charged pion and kaon decay. These processes become important at energies below the critical energy, i.e. the energy for which the meson interaction and decay lengths are nearly the same. In particular the critical energy for π decay is around 150 GeV, while the one for K is about ten times larger. From these considerations, it is clear that the $\mu^{\pm}$ number is particularly sensitive to a good description of the hadronic physics processes at low energies. We emphasize that we refer indeed to $\mu^{\pm}$ with energy down to 1 GeV. On the other hand, $\mu^{\pm}$ with energies around hundreds or thousands GeV in the atmosphere deeply penetrate the rock, and can be selected and detected by underground detectors. Multi-μ and μ-bundle events have also been studied with FLUKA, which has provided a succesful reproduction of experimental data [7].

To better identify the longitudinal shape of the shower components, detailed maps of fluences and energy deposition have been built. In Fig. 5 and 6 the fluences of $e^{\pm}$ and $\mu^{\pm}$ from the top of the atmosphere, down to the Earth's surface, are shown for Fe induced vertical showers at 10^{13} and 10^{15} eV. From the figures, it is evident that in the top part of the atmosphere the $e^{\pm}$ shower profile is more extended than the $\mu^{\pm}$ one, and that some $e^{\pm}$ can even propagate from lower altitudes towards higher ones. At the considered energies,

some $e^{\pm}$ and $\mu^{\pm}$ from the same shower can reach ground within a few km. Anyway, the largest fluences are found for both kind of particles in the spatial region located within $\sim$ 2 - 8 km above the Earth's surface, at distances not larger than 500 - 700 m from the shower axis. In Fig. 7 detailed maps of electromagnetic energy deposition for vertical Fe showers at 10^{13} and 10^{15} eV are presented. These maps are strictly related to the ones for e fluence shown in Fig. 5, already discussed. $e^{\pm}$ production thresholds have been set to 1 MeV, while γ threshold has been set to 0.5 MeV in our simulations.

The (N_e, N_{μ}) correlations for p and Fe showers at sea level and at 4000 m a.s.l. are shown in Fig. 8 and Fig. 9, respectively. Results for primary energies from 10^{12} to 10^{15} eV are plotted. It appears that for lower energy showers and higher altitudes it is more difficult to distinguish the primary spectrum composition on the basis of (N_e, N_{μ}) detection.

The features of EAS predicted by our simulations are in a qualitative agreement with those obtained by other authors. As a further step in our investigation, we plan to compare in more detail our theoretical results with those obtained by means of other models, e.g. those available in the CORSIKA code. Beyond the question of the comparison of hadronic interaction models, this can be helpful to identify also possible differences coming from different e.m. or transport models.

4. Acknowledgments

REFERENCES

1. D. Heck *et al.*, Report FZKA 6019 (1998)
2. A. Ferrari *et al.*, CERN Yellow Report 2005–10 (2005), INFN/TC_05/11, 1-387
3. A. Fassò *et al.*, Proc. of the CHEP2003 conference, La Jolla, CA, USA, March 24-28, 2003, (paper MOMT005) eConf C0303241 (2003), hep-ph/0306267
4. S. Roesler, R. Engel, J. Ranft, Proc. Monte-Carlo 2000 Conference, Lisboa, 23 - 26 October 2000, Springer Verlag eds. (2001), 1033
5. J. Ranft, Phys. Rev. D **51** (1995), 64-84
6. G. Battistoni *et al.*, Astropart. Phys. **12** (2000), 315-333
7. G. Battistoni *et al.*, Proc. of the NOW 2006 Workshop, to be published in Nucl. Phys. B(Proc. Suppl.).
8. G. Battistoni, A. Ferrari, M. Pelliccioni and R. Villari, Rad. Prot. Dosim. **112** (2004), 331-343; Adv. Space Res. **36** (2005), 1645-1652
9. S. Roesler, W. Heinrich and H. Schraube, Radiation Research 149 (1998) 87 ; Radiation Protection Dosimetry **98** (2002) 367-388
10. F. Ballarini *et al.*, J. of Physics: Conf. Series **41** (2006), 135-142
11. A. Fassò *et al.*, Proc. MonteCarlo 2000 Conference, Lisboa, 23 - 26 October 2000, Springer Verlag eds. (2001), 159-164
12. M. Antonelli *et al.*, Proc. VI Int. Conf. on Calorimetry in High Energy Physics (Calor 96), Frascati (Italy), 8–14 June 1996. Frascati Physics Series Vol. VI (1997), 561-570
13. G. Battistoni *et al.*, Nucl. Instr. Meth. **A394** (1997), 136–145
14. A. Ferrari and P.R. Sala, Proceedings of Workshop on Nuclear Reaction Data and Nuclear Reactors Physics, Design and Safety, A. Gandini, G. Reffo eds., Trieste, Italy, April 1996, **2** (1998), 424-532
15. A. Capella, U. Sukhatme, C.I. Tan, J. Tran Thanh Van, Phys. Rep. **236** (1994), 225
16. G. Collazuol *et al.*, NIM A **449** (2000), 609.
17. J. Ranft, S. Ritter, Acta Phys. Pol. B **11** (1980), 259; S. Ritter, Comput. Phys. Commun. **31** (1984), 393
18. G. Battistoni *et al.*, Proc. 11th Int. Conf. on Nuclear Reaction Mechanisms, Varenna, 12 - 16 June 2006, E. Gadioli ed. (2006), 483-495
19. M.G. Catanesi *et al.*, Nucl. Phys. **B732** (2006), 1-45
20. C. Alt *et al.*, arXiv:hep-ex/0606028
21. T. Sjöstrand, CERN Report CERN/TH 7112/93 (unpublished).
22. A. Ferrari *et al.*, Z. Phys. **C70** (1996), 413-426
23. A. Ferrari *et al.*, Z. Phys. **C71** (1996), 75-86